

Research Article

Collision and Stable Regions around Bodies with Simple Geometric Shape

A. A. Silva,^{1,2,3} O. C. Winter,^{1,2} and A. F. B. A. Prado^{1,2}

¹ *Space Mechanics and Control Division (DMC), National Institute for Space Research (INPE), São José dos Campos 12227-010, Brazil*

² *UNESP, Universidade Estadual Paulista, Grupo de Dinâmica Orbital & Planetologia, Av. Ariberto Pereira da Cunha, 333-Guaratinguetá 12516-410, Brazil*

³ *Universidade do Vale do Paraíba (CT I / UNIVAP), São José dos Campos 12245-020, Brazil*

Correspondence should be addressed to A. A. Silva, aurea.as@yahoo.com.br

Received 29 July 2009; Accepted 20 October 2009

Recommended by Silvia Maria Giuliatti Winter

We show the expressions of the gravitational potential of homogeneous bodies with well-defined simple geometric shapes to study the phase space of trajectories around these bodies. The potentials of the rectangular and triangular plates are presented. With these expressions we study the phase space of trajectories of a point of mass around the plates, using the Poincaré surface of section technique. We determined the location and the size of the stable and collision regions in the phase space, and the identification of some resonances. This work is the first and an important step for others studies, considering 3D bodies. The study of the behavior of a point of mass orbiting around these plates (2D), near their corners, can be used as a parameter to understand the influence of the gravitational potential when the particle is close to an irregular surface, such as large craters and ridges.

Copyright © 2009 A. A. Silva et al. This is an open access article distributed under the Creative Commons Attribution License, which permits unrestricted use, distribution, and reproduction in any medium, provided the original work is properly cited.

1. Introduction

The aim of this paper is to study the phase space of trajectories around some homogeneous bodies with well-defined simple geometric shapes. Closed-form expressions derived for the gravitational potential of the rectangular and triangular plates were obtained from Kellogg [1] and Broucke [2]. They show the presence of two kinds of terms: logarithms and arc tangents. With these expressions we study the phase space of trajectories of a particle around two different bodies: a square and a triangular plates. The present study was made using the Poincaré surface of section technique which allows us to determine the location and size of the stable and chaotic regions in the phase space. We can find the periodic, quasiperiodic and chaotic orbits.

Some researches on this topic can be found in Winter [3] that study the stability evolution of a family of simply periodic orbits around the Moon in the rotating Earth-Moon-particle system. He uses the numerical technique of Poincaré surface of section to obtain the structure of the region of the phase space that contains such orbits. In such work it is introduced a criterion for the degree of stability. The results are a group of surfaces of section for different values of the Jacobi constant and the location and width of the maximum amplitude of oscillation as a function of the Jacobi constant. Another research was done by Broucke [4] that presents the Newton's law of gravity applied to round bodies, mainly spheres and shells. He also treats circular cylinders and disks with the same methods used for shells and it works very well, almost with no modifications. The results are complete derivations for the potential and the force for the interior case as well as the exterior case.

In Sections 2 and 3, following the works of Kellogg [1] and Broucke [2], we show the expressions for the potential of the rectangular and triangular plates, respectively. In Section 4 we use the Poincaré surface of section technique to study the phase space around the plates. In Section 5 we show the size and location of stable and collision regions in the phase space. In the last section, we have some final comments.

2. The Potential of the Rectangular Plate

Let us consider a homogeneous plane rectangular plate and an arbitrary point $P(0, 0, Z)$, not on the rectangle. Take x and y axes parallel to the sides of the rectangle, and their corners referred to these axes are $A(b, c)$, $B(b', c)$, $C(b', c')$, and $D(b, c')$. Let ΔS_k denote a typical element of the surface, containing a point Q_k located in the rectangular plate with coordinates (x_k, y_k) . See Figure 1.

The potential of the rectangular plate can be given by the expression

$$\begin{aligned} U &= \frac{G\sigma\Delta S_k}{r_k} = G\sigma \int_c^{c'} \int_b^{b'} \frac{dx dy}{\sqrt{x^2 + y^2 + Z^2}} \\ &= G\sigma \left\{ \int_c^{c'} \ln \left(b' + \sqrt{b'^2 + y^2 + Z^2} \right) dy - \int_c^{c'} \ln \left(b + \sqrt{b^2 + y^2 + Z^2} \right) dy \right\}, \end{aligned} \quad (2.1)$$

where G is the Newton's gravitational constant, σ is the density of the material, and r_k is the distance between the particle and the point Q_k .

In evaluating the integrals we find

$$\begin{aligned} U &= G\sigma \left[c' \ln \frac{(b' + d_3)}{(b + d_4)} + c \ln \frac{(b + d_1)}{(b' + d_2)} + b' \ln \frac{(c' + d_3)}{(c + d_2)} + b \ln \frac{(c + d_1)}{(c' + d_4)} \right. \\ &\quad \left. + Z \left(\tan^{-1} \frac{b \cdot c'}{Z \cdot d_4} - \tan^{-1} \frac{b' \cdot c'}{Z \cdot d_3} + \tan^{-1} \frac{b' \cdot c}{Z \cdot d_2} - \tan^{-1} \frac{b \cdot c}{Z \cdot d_1} \right) \right], \end{aligned} \quad (2.2)$$

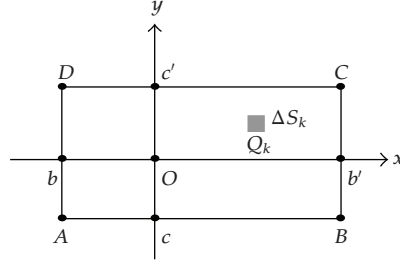


Figure 1: Rectangular plate is on the plane (x, y) .

where

$$\begin{aligned}
 d_1^2 &= b^2 + c^2 + Z^2, \\
 d_2^2 &= b'^2 + c^2 + Z^2, \\
 d_3^2 &= b^2 + c'^2 + Z^2, \\
 d_4^2 &= b'^2 + c'^2 + Z^2
 \end{aligned} \tag{2.3}$$

are the distances from $P(0, 0, Z)$ to the corners $A, B, C,$ and $D,$ respectively.

3. The Potential of the Triangular Plate

We will give the potential at a point $P(0, 0, Z)$ on the Z -axis created by the triangle shown in Figure 2 located in the xy -plane. The side $\overline{P_1P_2}$ is parallel to the x -axis. The coordinates of P_1 and P_2 are $\vec{r}_1(x_1, y_1)$ and $\vec{r}_2(x_2, y_2)$, but we have that $y_1 = y_2$ and $x_1 > x_2 > 0$. The distances are given by $d_1^2 = x_1^2 + y_1^2 + Z^2$ and $d_2^2 = x_2^2 + y_1^2 + Z^2$, where d_1 is the distance from $P(0, 0, Z)$ to the corner $P_1(x_1, y_1)$ and d_2 is the distance from $P(0, 0, Z)$ to the corner $P_2(x_2, y_1)$. Using the definition of the potential, we have that the potential at $P(0, 0, Z)$ can be given by

$$U = G\sigma \left\{ y_1 \ln \left[\frac{x_1 + d_1}{x_2 + d_2} \right] + Z \tan^{-1} \left(\frac{\beta_1 Z}{d_1} \right) - Z \tan^{-1} \left(\frac{\beta_2 Z}{d_2} \right) - |Z| \alpha_{12} \right\}, \tag{3.1}$$

where $\beta_1 = x_1/y_1$, $\beta_2 = x_2/y_2$, and $\alpha_{12} = \alpha_1 - \alpha_2$ represent the angle of the triangle at the origin O and it is showed in Figure 2.

The potential of this triangle at the point $P(0, 0, Z)$ on the Z -axis must be invariant under an arbitrary rotation of the triangle around the same Z -axis. Therefore, (3.1) should also be invariant under this rotation and their four terms are individually invariant, where they can be expressed in terms of invariant quantities, such as the sides and the angle of the triangle. The potential of an arbitrary triangular plate $P_1P_2P_3$ (Figure 3) can be obtained by

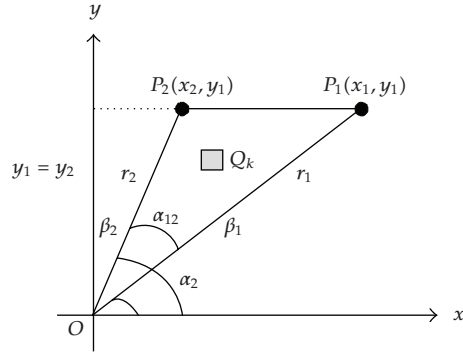


Figure 2: Triangle $\overline{OP_1P_2}$ located in the xy -plane (x, y) .

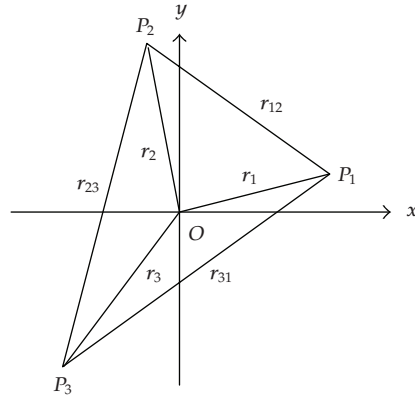


Figure 3: Triangular plate $\overline{P_1P_2P_3}$.

the sum of three special triangles of the type used in this section. So, the result will have three logarithmic terms and three arc-tangent terms. So, the potential is given by

$$U = G\sigma \left\{ \frac{C_{12}}{r_{12}} \ln \left[\frac{d_1 + d_2 + r_{12}}{d_1 + d_2 - r_{12}} \right] + \frac{C_{23}}{r_{23}} \ln \left[\frac{d_2 + d_3 + r_{23}}{d_2 + d_3 - r_{23}} \right] + \frac{C_{31}}{r_{31}} \ln \left[\frac{d_3 + d_1 + r_{31}}{d_3 + d_1 - r_{31}} \right] \right. \\ \left. + \tan^{-1} \left(\frac{Nd_1}{D_1} \right) + \tan^{-1} \left(\frac{Nd_2}{D_2} \right) + \tan^{-1} \left(\frac{Nd_3}{D_3} \right) + \text{Sign}(Z)\pi \right\}, \quad (3.2)$$

where the numerator and the denominators are

$$N = -Z(C_{12} + C_{23} + C_{31}), \\ D_1 = Z^2(r_1^2 + D_{23} - D_{31} - D_{12}) - C_{12}C_{31}, \\ D_2 = Z^2(r_2^2 + D_{31} - D_{12} - D_{23}) - C_{23}C_{12}, \\ D_3 = Z^2(r_3^2 + D_{12} - D_{23} - D_{31}) - C_{31}C_{23}. \quad (3.3)$$

The symbol $\text{Sign}(Z)$ in (3.2) is the sign of the variable Z and r_{ij} ($i, j = 1, 2, 3$) is the distance between P_i and P_j . In particular, the dot-product $D_{ij} = r_i r_j \cos \alpha_{ij}$ and the cross-product $C_{ij} = r_i r_j \sin \alpha_{ij}$ of the vectors \mathbf{r}_i and \mathbf{r}_j are two invariants, where $\alpha_{ij} = \alpha_i - \alpha_j$. In order to obtain more details see Broucke [2]. This result is invariant with respect to an arbitrary rotation around the Z -axis.

An important generalization of (2.2) and (3.2) can be done, for the case where the point P has arbitrary coordinates (X, Y, Z) instead of being on the Z -axis. For the rectangle, this task is rather easy, because the four vertices $A, B, C,$ and D have completely arbitrary locations. In order to have more general results it is sufficient to replace (b, b', c, c') by $(b - X, b' - X, c - Y, c' - Y)$ in (2.2). For the triangle, it is sufficient to replace all the vertex-coordinates (x_i, y_i) by $(x_i - X, y_i - Y)$ in (3.2). These generalizations give us expressions for the potential U of the rectangle and the triangle as a function of the variables (X, Y, Z) . Then, it is possible to compute the components of the acceleration by taking the gradient of the potential. It is important to note that, in taking the partial derivatives of $U(X, Y, Z)$, the arguments of the logarithms and the arc tangents were treated as constants by Broucke [2]. This simplifies the work considerably. The general expressions of the acceleration allow us to study orbits around these plates, and this study is very important to obtain knowledge that will be necessary to study the cases of three-dimensional solids, such as polyhedra.

4. Study of the Phase Space around Simple Geometric Shape Bodies

With the potential determined, we study the phase space of trajectories of a point of mass around the plates. In this section we use the Poincaré surface of section technique to study the regions around the rectangular and triangular plates. In this part of the paper we explore the space of initial conditions. The results are presented in Poincaré sections (x, \dot{x}) , from which one can identify the nature of the trajectories: periodic, quasiperiodic, or chaotic orbits. We can find the collision regions and identify some resonances.

In order to obtain the orbital elements of a particle at any instant it is necessary to know its position (x, y) and velocity (\dot{x}, \dot{y}) that corresponds to a point in a four dimensional phase space. The conservation of the total energy of the system implies in the existence of a three-dimensional surface in this phase space. For a fixed value of the total energy only three of the four quantities are needed, for example, $x, y,$ and \dot{x} , since the other one \dot{y} is determined, up to the sign, by the total energy. By defining a plane, that we choose $y = 0$, in the resulting three-dimensional space, the values of x and \dot{x} can be plotted every time the particle has $y = 0$. The ambiguity of the sign of \dot{y} is removed by considering only those crossing with a fixed sign of \dot{y} . The section is obtained by fixing a plane in the phase space and plotting the points when the trajectory intersects this plane in a particular direction (Winter and Vieira Neto, [5]). This technique is used to determine the regular or chaotic nature of the trajectory. In the Poincaré map, if there are closed well-defined curves then the trajectory is quasiperiodic. If there are isolated single points inside such islands, the trajectory is periodic. Any "fuzzy" distribution of points in the surface of section implies that the trajectory is chaotic (Winter and Murray [6]).

In order to study the regions around simple geometric shape bodies, two cases were considered. In the first case we used a square plate, where all of its sides are $\ell = 2$ and the initial position of the test particle is chosen arbitrarily in the right side of the plate. The motion of the particle is in the counterclockwise direction. In the second case we used an equilateral triangular plate, with sides $\ell = 1$ and one of its sides is parallel to the y -axis. For the triangle, the initial position of the test particle is in the right side of the plate and its motion is in the

counterclockwise direction. Both of the cases consider a baricentric system, where the plates are centered in the origin of the system. The constants used are the Newton's gravitational constant and the density of the material, respectively, $G = \sigma = 1$.

In this paper, the Poincaré surface of section describes a region of the phase space for two-body problem (plate-particle). The numerical study makes use of the Burlisch-Stoer method of integration with an accuracy of $O(10^{-12})$. The Newton-Raphson method was used to determine when the trajectory crosses the plane $y = 0$ with an accuracy of $O(10^{-11})$. There is always a choice of surfaces of section and, in our work, the values of x and \dot{x} were computed whenever the trajectory crossed the plane $y = 0$ with $\dot{y} > 0$.

In this section, Figure 4 represents a set of Poincaré surfaces of section around the triangular plate with values of energy, E , varying from -0.41 to -0.46 , at intervals of 0.01 . We considered approximately seventy starting conditions for each surface of section, but most of them generated just a single point each one. In that case the particle collided with the plate.

Figures 4(a) to 4(f) show regions where the initial conditions generated well-defined curves. These sections represent quasiperiodic trajectories around the triangular plate. The center of the islands for each surface of section corresponds to one periodic orbit of the first kind (circular orbit). In Figure 4(a), for example, we can see a group of four islands corresponding to a single trajectory with $E = -0.41$ and $x_0 = -0.8422$. The center of each one of those islands corresponds to one periodic orbit of the second kind (resonant orbit). In the same figure there is a separatrix that represents the trajectory with $E = -0.41$ and $x_0 = -0.83176$ where the particle has a chaotic movement confined in a small region. Figure 4(d) shows that the group of four islands is disappearing and a new group of five islands appears. This new group of islands corresponds to a trajectory with $E = -0.44$ and $x_0 = -0.80281$. The region of single points outside the islands corresponds to a chaotic "sea" where the particle collides with the plate. This is a region highly unstable.

Figure 5(a) shows a Poincaré surface of section around the triangular plate for energy, $E = -0.4$. With a zoom in the region 1 we can see a fuzzy but confined distribution of points that corresponds to the separatrix (Figure 5(b)) generated with $x_0 = -0.80816$. With a zoom in the region 2 we can see islands (Figure 5(c)) that were generated with $x_0 = -0.81596$ and $x_0 = -0.83351$.

A similar structure of the phase space is found for the square plate when analyzed its Poincaré surface of section.

5. Collision and Stable Regions

In this section we show a global vision of the location and size of the stable and collision regions around the triangular and square plates, using Poincaré map. The values of x , when $\dot{x} = 0$, are measured with the largest island of stability (quasiperiodic orbit) for each value of energy (Winter [3]). With the diagrams (Figures 6 and 7) we can see the evolution of the stability for the family of periodic orbits for different values of energy constant.

The surfaces of section are plotted at intervals of 0.02 for the energy constant (E). For the triangular plate, the energy varies from -0.01 to -0.47 and, for the square plate, from -0.13 to -1.09 . The values of the energy ($E = -0.47$) for the triangle and ($E = -1.09$) for the square represent the region that there is no island of stability within the adopted precision.

Figure 6(a) shows the stable and collision regions around the triangular plate. The white color represents the region that is considered stable, neglecting the small chaotic regions that appear in the separatrices. The collision region is represented by the dark gray color and it indicates the region where the particle collides with the plate due to its

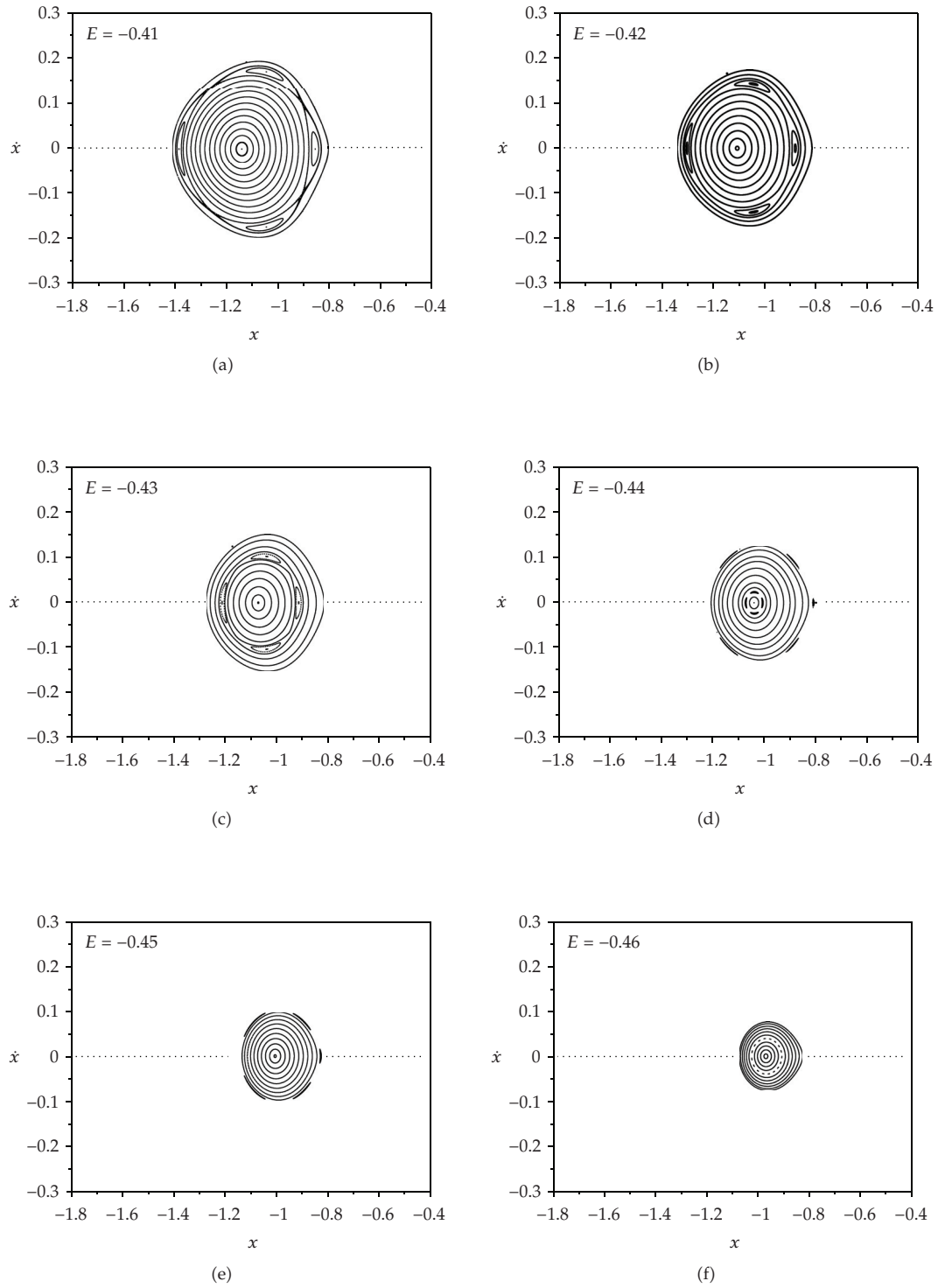
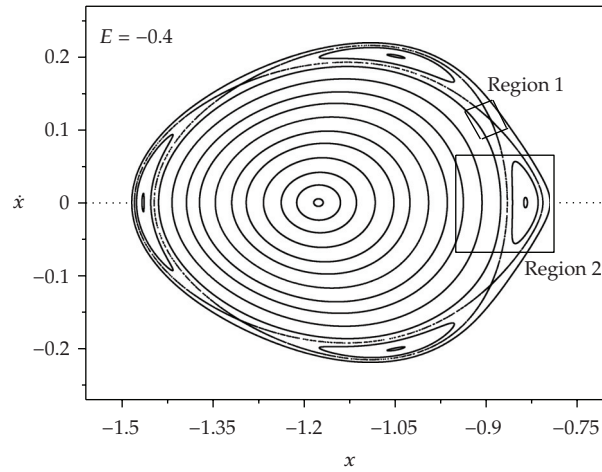
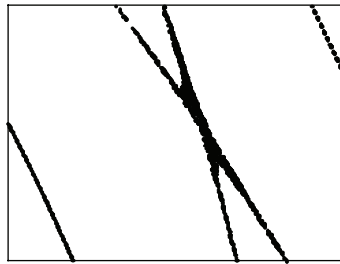


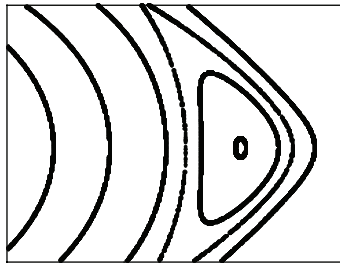
Figure 4: A group of Poincaré surfaces of section of trajectory around the triangular plate for different values of energy, $-0.46 \leq E \leq -0.41$ at intervals of 0.01.



(a)



(b)



(c)

Figure 5: (a) Poincaré surfaces of section around the triangular plate for energy, $E = -0.4$; (b) a zoom in region 1 that represents the separatrix; (c) a zoom in region 2 that represents a group of islands.

gravitational attraction. The light gray color corresponds to a “prohibited” region where there are no starting conditions for those values of energy. The triangular plate is located to the right of the limit of the collision border. Figure 6(b) corresponds to a zoom of the previous one in order to have the best visualization of the regions.

Figure 7(a) summarizes the same studies around the square plate and the color codes are the same as mentioned for the triangle. The square plate is located to the left of the limit of the collision border. Figure 7(b) corresponds to a zoom of the previous one.

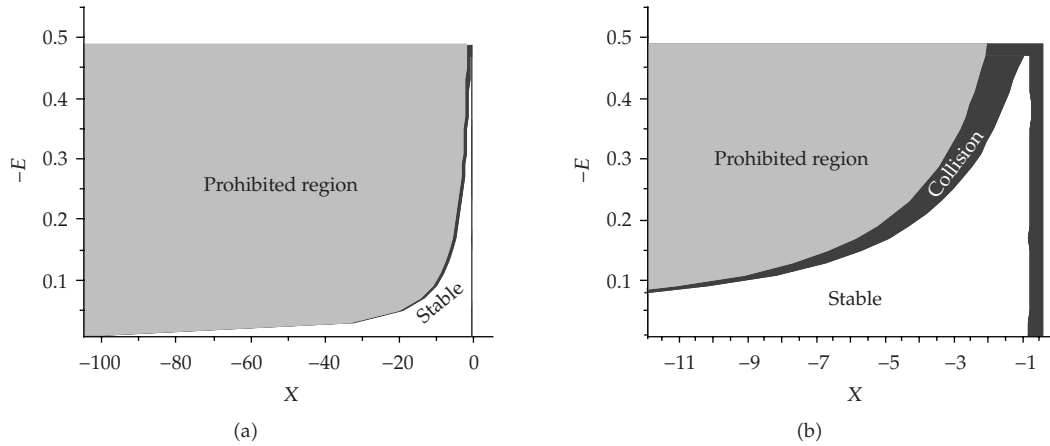


Figure 6: (a) Study of the regions around the triangular plate: stable area (white), collision area (dark gray), and “prohibited” area (light gray); (b) zoom of a region in (a).

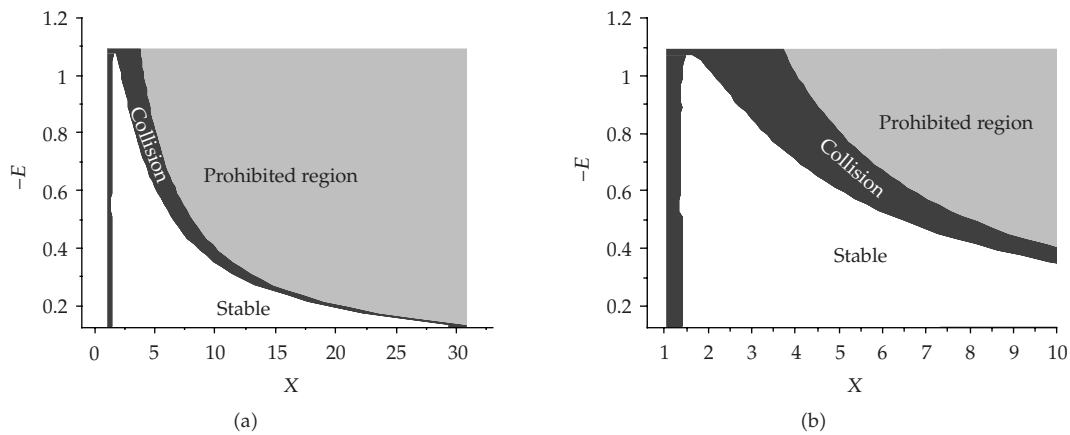


Figure 7: (a) Study of the regions around of the square plate: stable area (white), collision area (dark gray), and “prohibited” area (light gray); (b) zoom of a region in (a).

6. Trajectories around Triangular and Square Plates

In the last section was shown a global vision of a family of orbits around the geometric plates. In this section we will show some trajectories of a particle around triangular and square plates. The initial conditions (position and velocity) of the particle that orbit the plates are given by:

$$\begin{aligned} (x, y, z) &= (x_0, 0, 0), \\ (V_x, V_y, V_z) &= \left(0, -\sqrt{2(E + U)}, 0\right), \end{aligned} \tag{6.1}$$

where E is the total energy of the system and U is the potential energy generated by the plate.

Table 1: Value of the energy (E) and the initial position of the particle (x_0) for the triangular and square plates.

Figures	E	x_0
8	-0.40	-0.83
9	-0.41	-0.83176
10	-0.60	1.4

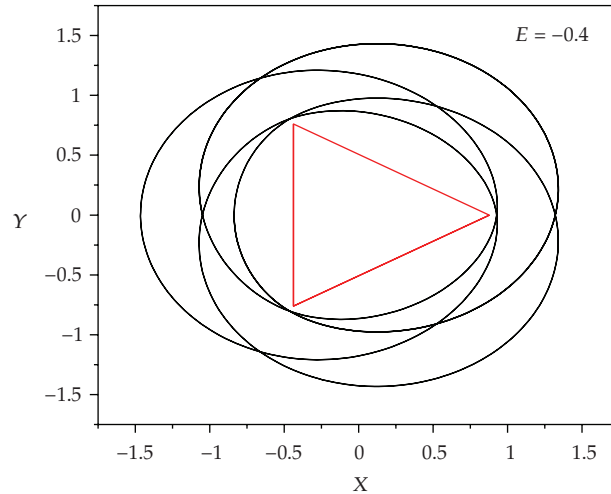
**Figure 8:** Trajectory around the triangular plate: quasiperiodic.

Table 1 shows the value of the initial position of the particle (x_0) and its correspondent value of the energy for each trajectory around the triangular and square plates. Figures 8 and 9 show a quasiperiodic orbit and a chaotic orbit (in a region of the separatrix), respectively, around the triangular plate. Figure 10 shows a quasiperiodic orbit around the square plate.

The trajectories in these figures show that the effect of the potential due to the plates can be compared with the effect of the Earth's flattening (J_2), generating trajectories as a precessing elliptic orbit.

In this section we will explore the regions very close to the vertex of the geometric plates and verify the behavior of the particle in this situation due to the potentials of the plates. So, it is showed an analysis of the semimajor axis and the eccentricity of the orbit.

In the next example is considered a triangular plate as a central body, the value of the energy is $E = -0.1$ and the initial position for the particle is $x_0 = -1.14$ and $y_0 = z_0 = 0$, that generate a quasiperiodic orbit. Figure 11 shows the trajectory around the plate, where A , B , and C are the vertexes of the triangular plate and Figure 12 shows the behavior of the semimajor axis versus time. The points in Figure 11 correspond to the enumerated regions in Figure 12. For better visualization of Figure 11, there is a zoom of the region around the plate. Figure 13 shows a zoom of Figure 12 with the details of the semimajor axis peaks along six orbital periods. The results show the following features.

The codes 1a, 2a, 3a, 4a, 5a, and 6a are the maximum values of the semimajor axis that occur when the particle is close to the vertex A during six complete orbits. The codes 1 to 6 correspond to the six close approaches of the particle to the vertex A . The results show that

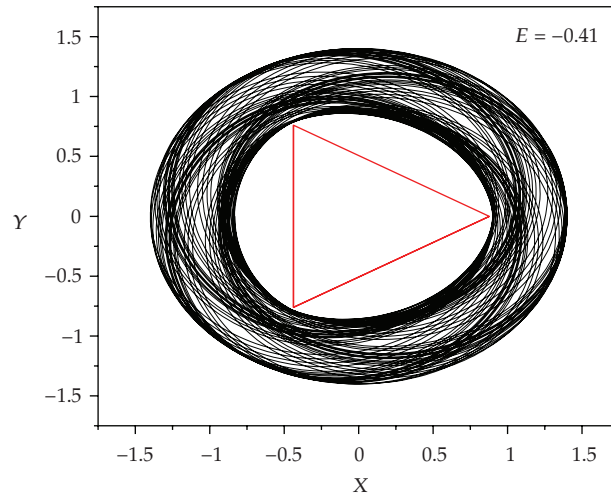


Figure 9: Trajectory around the triangular plate: chaotic orbit (separatrix).

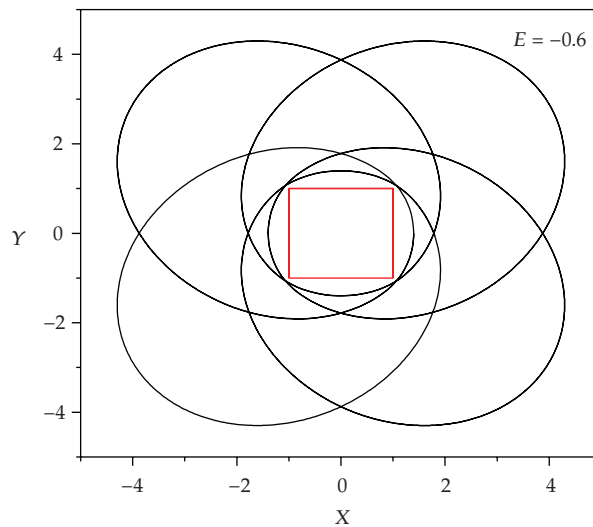


Figure 10: Trajectory around the square plate: quasiperiodic.

the semimajor axis increases as the particle approaches to the vertex A . From Figures 11 to 13 we see the same codes for passages of the particle close to the other two vertices, B and C . Since the trajectory of the particle does not get so close to the vertices, B and C , then the increase on the semimajor axis is not so large in these cases.

With these analyses we can verify that the proximity of the particle to the corners of the plate changes the behavior of the trajectory. In the studied cases, the orbits become eccentric and precess. For the eccentricity we could verify a similar behavior as that found for the semimajor axis.

The studies with the square plate show the same behavior as obtained for the triangle.

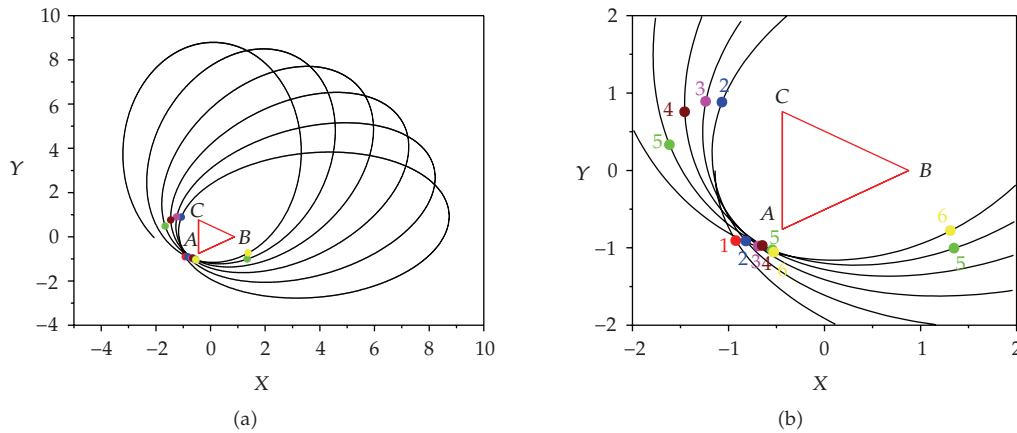


Figure 11: (a) Trajectory of the particle around the triangular plate. (b) Zoom of the trajectory near the plate.

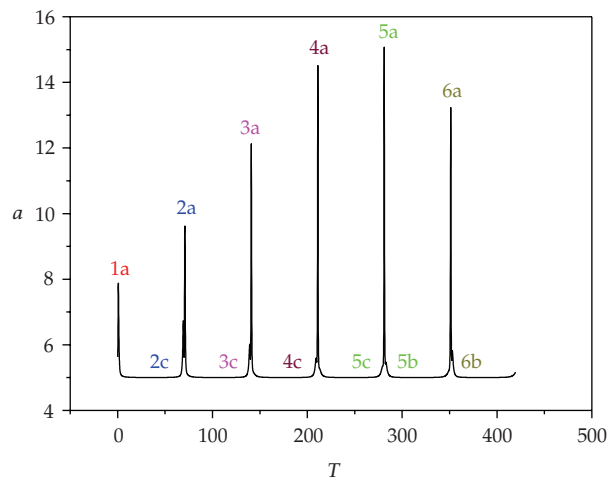


Figure 12: Semimajor axis of the orbit.

7. Final Comments

In this paper we used closed form solutions for the gravitational potential for two simple geometric shape bodies in order to study the behavior of a particle around each one of them. The development was applied to the square and to the triangular plates. We used the Poincaré surface of section technique to study the phase space of trajectories of a particle around those plates. We identified different kinds of orbits: periodic, quasiperiodic, and chaotic orbits. We found a collision region and identified some resonances.

The results showed that there is a region of starting conditions where it is possible to have orbits around the plates before the collision. The location and size of the stable and collision regions were measured for each value of energy and it showed us the evolution of the stable regions in the phase space. We have seen that the Poincaré surface of section technique is an easy and powerful way to identify the nature of the orbits.

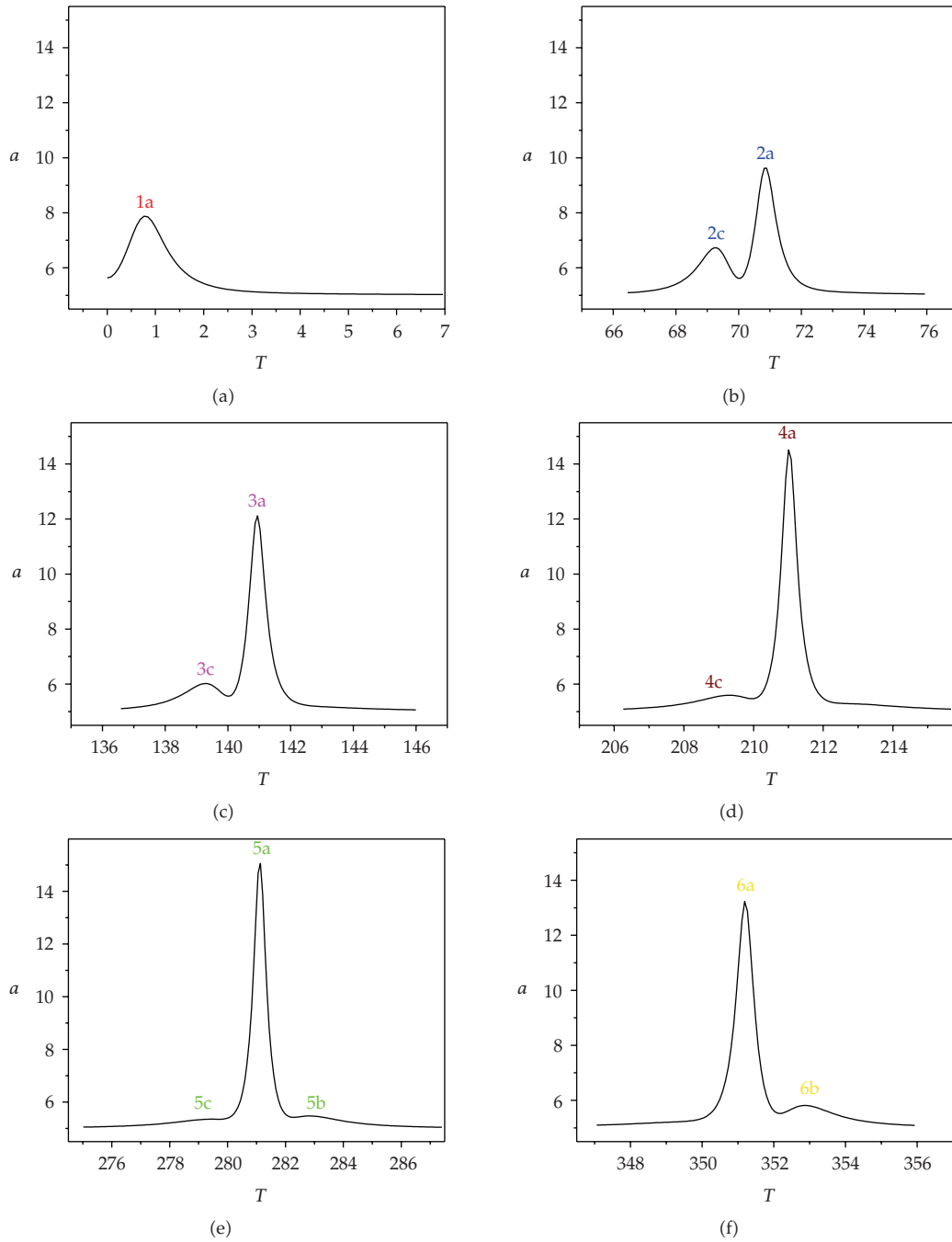


Figure 13: Zoom of Figure 12. Peak of semimajor axis in six orbital periods.

It was observed that the corners of the plates have a significant influence in the behavior of the trajectory, mainly when the particle has a close approach to them. The orbits become eccentric and precess due their gravitational field.

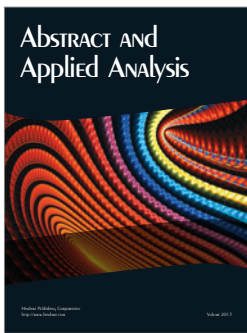
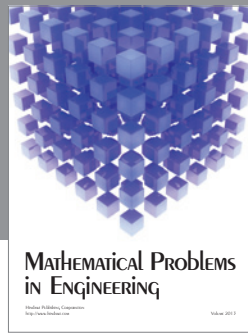
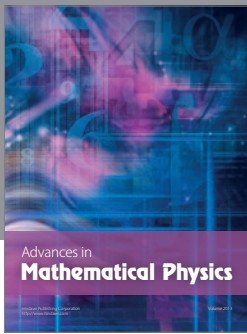
This study opens the way to obtain the potential and the trajectories around three-dimensional bodies with irregular shapes, such as asteroids and comets.

Acknowledgment

The authors wish to express their appreciation for the supports provided by the Brazilian agencies: FAPESP, CAPES, and CNPq. They are very grateful to Roger A. Broucke for the information and discussions.

References

- [1] O. D. Kellogg, *Foundations of Potential Theory*, Dover, New York, NY, USA, 1929.
- [2] R. A. Broucke, "Closed form expressions for some gravitational potentials: triangle, rectangle, pyramid and polyhedron," in *Proceedings of AAS/AIAA Spaceflight Mechanics Meeting*, Albuquerque, NM, USA, February 1995.
- [3] O. C. Winter, "The stability evolution of a family of simply periodic lunar orbits," *Planetary and Space Science*, vol. 48, no. 1, pp. 23–28, 2000.
- [4] R. A. Broucke, "The gravitational attraction of spheres and spherical shells," in *Advances in Space Dynamics*, O. C. Winter and A. F. B. A. Prado, Eds., vol. 2, pp. 190–233, INPE, São José dos Campo, Brazil, 2002.
- [5] O. C. Winter and E. Vieira Neto, "Distant stable direct orbits around the Moon," *Astronomy and Astrophysics*, vol. 393, no. 2, pp. 661–671, 2002.
- [6] O. C. Winter and C. D. Murray, *Atlas of the Planar, Circular, Restricted Three-Body Problem. I. Internal Orbit*, vol. 16 of *QMW Maths Notes*, Queen Mary and Westfield College, London, UK, 1994.



Hindawi

Submit your manuscripts at
<http://www.hindawi.com>

